J. Plasma Fusion Res. SERIES, Vol. 4 (2001) 583–586

Boundary Condition May Change Chaos

ITOH Sanae-I.*, KAWAI Yoshinobu[1] and YAGI Masatoshi
RIAM, Kyushu University, Kasuga 816-8580 Japan
[1]*Interdisciplinary Graduate School of Engineering Sciences, Kyushu University, Kasuga 816-8580 Japan*

(Received: 5 December 2000 / Accepted: 27 August 2001)

Abstract

Role of boundary condition for the appearance of chaos is examined. Imposition of the boundary condition is interpreted as the reduction of the system size L. For a demonstration, Rayleigh-Benard instability is considered and the shell model analysis is applied. It is shown that the reduction of L reduces the number of positive Lyapunov exponent of the system, hence opens the route from the turbulence, to the chaos and to the limit cycle/fixed point.

Keywords:

chaos, ion-ion instability, Lyapunov exponent, Rayleigh-Benard instability, shell model

1. Introduction

There have been reported various routes to turbulent state in plasmas. Period doubling process due to Hopf bifurcation is a typical route which associates a chaos. Experimentally, a plasma of unstable system often reaches the turbulent state without going through the chaotic state. It has been found that the ion-ion instability in double plasma in the presence of ion beam component directly enters into the turbulent state [1]. On the contrary, when the bias grid is imposed at finite distance from the central mesh, the discrete spectrum of unstable wave with an intermittent behavior was found. This implies that a certain constraint upon the system (e.g., boundary condition) reduces the number of degrees of freedom. Hence the phase diagram, on which the route to turbulence is determined, may also be affected by the constraint.

In this paper, a working hypothesis is presented; the boundary condition is imposed by the bias grid, which makes the constraint for the number of unstable modes in between the central mesh and the imposed grid. If there are many unstable and independent modes, and many positive Lyapunov numbers exist, the system develops to the fully turbulent state. However, if the number of existing modes reduces and the positive Lyapunov number becomes small (say, unity), the system shows the chaotic behavior. And, the maximum Lyapunov exponent becomes zero, only a limit cycle solution exists. Imposition of the grid determines the number of unstable modes, from the fundamental to higher harmonics, for given plasma parameters. The gradual reduction of the distance between the grid and the central mesh cuts off the higher harmonics, so as to reduce the number of independent unstable modes. This mechanism has an analogy to the inverse process of period doubling (where the time period is replaced by the space wavelength).

For example, in the ion-beam system, the modes with $c_1 < k\lambda_D < c_2$ can become unstable, where k is the wave number, λ_D is the Debye length, and numerical constants satisfy $c_1 \simeq 0$, being controlled by the ion-neutral collisions, and c_2 is determined by the ion-Landau-damping, e.g., $c_2 \sim 1$ for the relevant parameters in [2]. Similar argument is applied to the Rayleigh-Benard instability, which corresponds to the flute mode in plasmas. Here, the Rayleigh-Benard instability is considered, since the mode becomes unstable in a finite

*Corresponding author's e-mail: s-iitoh@riam.kyshu-u.ac.jp

region of k-space, can develop into turbulence, and is sensitive to the constraint on the period of the system (in the perpendicular direction to the magnetic field).

In order to analyze the hypothesis of the basic mechanisms theoretically, we examine the route from the turbulence to the chaos and to the limit cycle/fixed point. We adopt a shell model analysis, by which we can extract all the turbulence, chaos and limit cycle/fixed point behavior [3]. The reduction of the system size is imposed, and the role of boundary condition on the appearance of chaos is shown below.

2. Model Equation

A simplified model, which describes Rayleigh-Benard turbulence in the fluid layer of height h under the gravity g is adopted. The temperature field is $T = T_0(x_3) + \theta$, $T_0(x_3) = T_0 - \beta x_3$ and the density is $\rho_0 = \rho_b(1 + \alpha\beta x_3)$, where θ is the fluctuating temperature, x_3 is the vertical distance from the bottom, α is the thermal expansion coefficient and ρ_b is the density at the bottom. The differential buoyancy is given by $\rho_b \alpha g \theta$.

Navier-Stokes equation for incompressible fluid and heat equation are written as

$$\nabla \cdot \boldsymbol{v} = 0, \tag{1}$$

$$\frac{\partial v_i}{\partial t} + (\boldsymbol{v}\cdot\nabla)v_i = -\frac{\partial p}{\partial x_i} + \nu\nabla^2 v_i + \alpha g\,\theta\delta_{i3} \tag{2}$$

$$\frac{\partial \theta}{\partial t} + (\boldsymbol{v}\cdot\nabla)\theta = \kappa\nabla^2\theta + \beta v_i \delta_{i3} \tag{3}$$

where ν is the kinematic viscosity, κ is the heat diffusivity, δ_{ij} is the Kronecker's delta and $i = 3$ represents the direction of buoyancy.

Applying the Fourier transformation, we rewrite eqs.(1)–(3) into the shell-model equations (see [3,4] for derivation). The nearest and the second nearest neighbor complex component model is given as

$$\frac{du_n}{dt} = i\left(k_n u^*_{n+1}u^*_{n+2} - k_{n-2}u^*_{n-1}u^*_{n+1} k_{n-3}u^*_{n-1}u^*_{n-2} \right) - P_r k_n^2 u_n + P_r p_n \tag{4}$$

$$\frac{dp_n}{dt} = i\Big\{ k_{n-1}\left(u^*_{n-1}p^*_{n+1} - u^*_{n+1}p^*_{n-1} \right) - k_{n-2}\left(u^*_{n-2}p^*_{n-1} + u^*_{n-1}p^*_{n-2} \right) + k_n\left(u^*_{n+1}p^*_{n+2} - u^*_{n+2}p^*_{n+1} \right)\Big\} - R_a u_n - k_n^2 p_n \tag{5}$$

where * represents the complex conjugate, $n = 1,\ldots,$ N is the number of each shell, $k_n = C2^{n-1}$, C is a numerical constant, u_n is the fluctuating velocity, p_n is the fluctuating temperature, R_a is the Rayleigh number, $R_a = h^4 g\alpha\beta/\kappa\nu$, and $P_r = \nu/\kappa$ is the Prandtl number. To derive these equations, $k \simeq k_3$ is assumed, and the normalizations are used: $kh \to k$, $k\kappa h^{-2} \to t$, $v_3 h/\kappa \to u$ and $\theta\alpha g h^3/\nu\kappa \to p$. The boundary conditions are given as $u_{-1} = u_0 = u_{N+1} = u_{N+2} = 0$ and $p_{-1} = p_0 = p_{N+1} = p_{N+2} = 0$, which ensure no interaction between N-shell and the vacuum outside of N-shells. If we neglect the third term in RHS of (4) and (5), and add the force terms to them, respectively, then eq.(4) corresponds to the GOY model [5,6] and eq.(5) corresponds to passive scalar field which involves with GOY model [7].

The linear stability analysis shows that the system is unstable if $R_a > k_n^4$. The growth rate increases with the increase of R_a and P_r. The reduction of R_a value corresponds to the reduction of the system size h. This reduces the number of unstable modes in the shell model. The analysis on this shell model of Eqs.(4) and (5) has been done and the turbulent , the chaotic and the limit cycle nature has been reported in refs. [3,4].

3. Analysis and Results

Here the nonlinear calculation is done for $C = 1.0$, N = 13 (or N = 14) and a simple phase diagram is plotted on $R_a - P_r$ plane (Fig.1). Heuristically, the higher R_a number region above the line shows the turbulence, and the limit cycle behavior with no positive Lyapunov exponent is found below the line. An imposition of

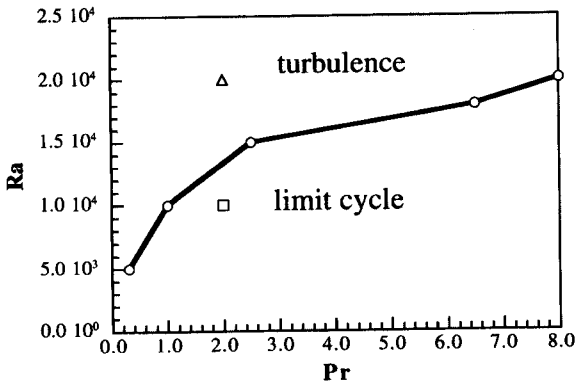

Fig. 1 Phase-diagram on $R_a - P_r$ plane. The higher R_a number region above the line shows the turbulence and the limit cycle behavior with no positive Lyapunov exponent is found below the line.

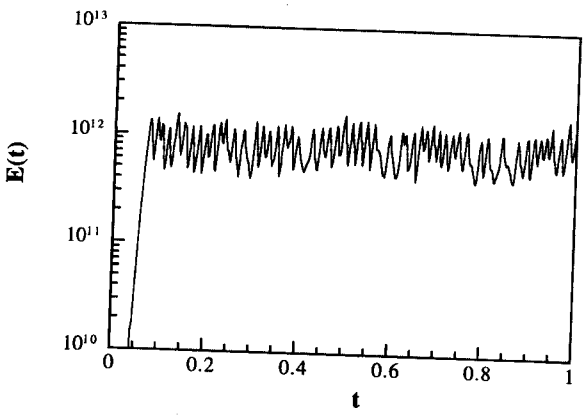

Fig. 2 (a) The temporal evolution of the total energy in the case with $P_r = 2.0$ and $R_a = 2.0 \times 10^4$.

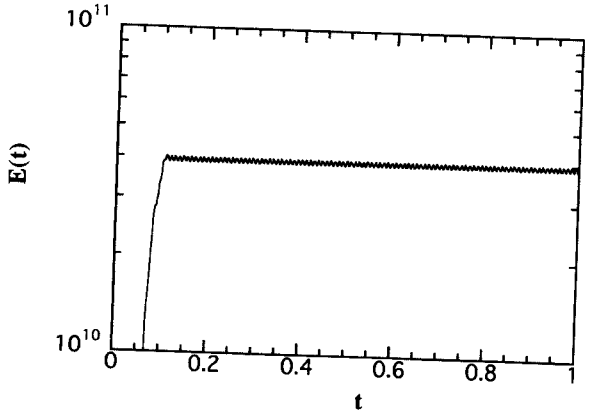

Fig. 3 (a) The temporal evolution of the total energy in the case with $P_r = 2.0$ and $R_a = 1.0 \times 10^4$.

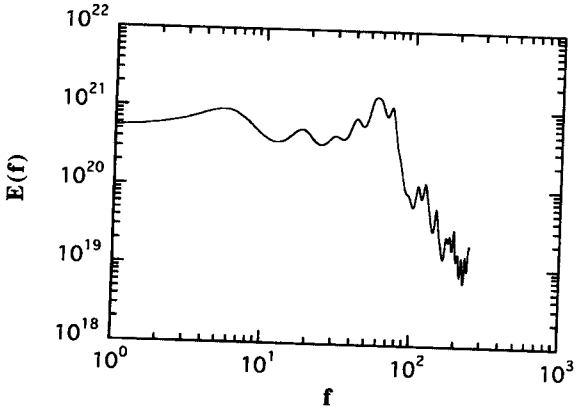

Fig. 2 (b) The power spectrum in the case with $P_r = 2.0$ and $R_a = 2.0 \times 10^4$.

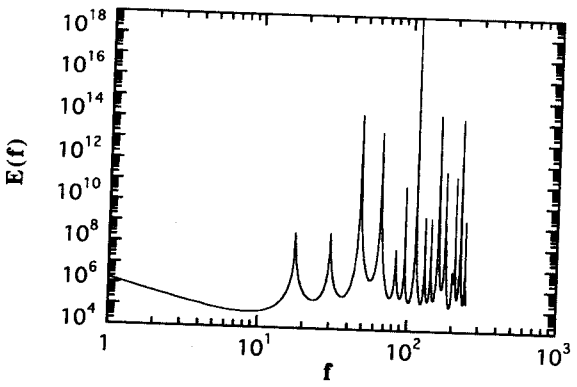

Fig. 3 (b) The power spectrum in the case with $P_r = 2.0$ and $R_a = 1.0 \times 10^4$.

boundary condition can be simulated by the reduction of the value R_a. Cases with $P_r = 2$ for $R_a = 2 \times 10^4$ and $R_a = 10^4$ are shown in Figs. 2 and 3, respectively. The temporal evolution of the total energy defined by

$$E(t) = \frac{1}{2} \sum_n \left(|u_n|^2 + |p_n|^2 \right) \qquad (6)$$

and the power spectrum are plotted. Two frequency spectra clearly show the difference between the turbulence and the limit cycle. The appearance of the limit cycle demonstrates the reduction of the number of degrees of freedom with positive Lyapunov exponent.

The reduction of system size h is also considered if R_a is kept constant and P_r number is increased. Such a case is shown in Fig.4. The maximum Lyapunov exponent vs P_r number (a) and the power spectra (b) for different values of $P_r = 2.5$ and 9 are plotted for $R_a = 2 \times 10^4$. The maximum Lyapunov exponent is positive in the region of $0.5 < P_r < 7.5$ and suddenly drops down to zero at $P_r = 8$, which corresponds to the phase boundary in the diagram (Fig.1).

For $P_r = 2$ and $P_r = 5$, the power spectra are fitted as $E(f) \sim f^{-3.15}$ and $E(f) \sim f^{-2.2}$, respectively, in the range of $1000 < f < 2500$. On the other hand, the period doubling cascade such as $f/16$, $f/18$, $f/4$ $f/2$ ...., where f is the initial frequency, is observed in the case of $P_r = 8$ [8]. This corresponds the fact that the fluctuation amplitude is very small and converges to the limit cycle.

The intermittency is analyzed, obtaining the scaling exponent of higher order spectrum function. For the case in Fig.4(b), the intermittency, which is observed by the deviation from the K41 prediction [9], is found for the case of $P_r = 2$ and $P_r = 5$. However, for $P_r \geq 8$, the intermittency disappears and the chaotic attractor does not exist.

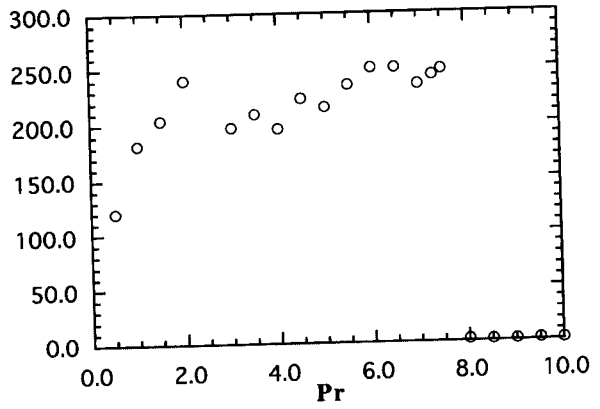

Fig. 4 (a) The log-log plot of the maximum Lyapunov exponent versus Prandtl number in the case of $R_a = 2.0 \times 10^4$.

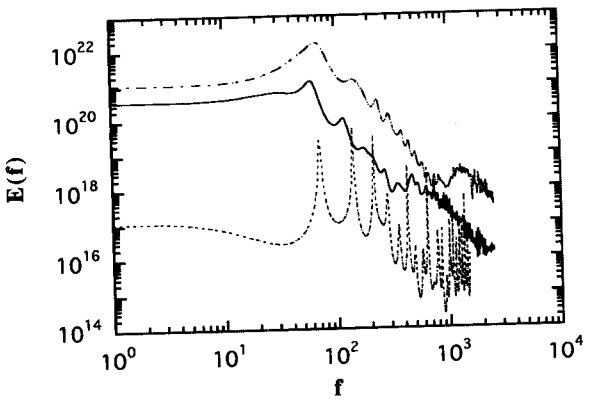

Fig. 4 (b) The log-log plot of power spectra of the total energy in the case of $R_a = 2.0 \times 10^4$. The solid line shows the power spectrum for $P_r = 2.0$, the dotted-dashed line is the case of $P_r = 5.0$ and the dotted line corresponds to the case of $P_r = 8.0$.

4. Summary

In this paper, we examined the role of boundary condition for the appearance of chaos. Imposition of the boundary condition is interpreted as the reduction of the system size. It is found that the reduction of the system size reduces the number of degrees of freedom associated with positive Lyapunov exponent. Below the boundary in Fig.1, only the limit cycle solution is found, this fact shows that there is no positive Lyapunov exponent. Well above the line, the turbulent state is realized. Close to the phase boundary in upper region, the chaotic behavior would be seen, which might be related with Ruelle-Takens scenario [10]. Further study of the behavior of solution and the number of positive Lyapunov exponent across the boundary may clarify the discrimination between the chaos and the turbulence. The role of system size on ion-ion instability can be considered in a similar way. In the cold plasma approximation, the parameter, $(1 + (\omega_{pb}/\omega_{pi})^{2/3})^3\omega_{pi}^2\nu_b^{-2}L^2 - \lambda_D^{-2}L^2$, may play the similar role to R_a-number. Reduction of the size L may open the route from the turbulence to the chaos and to the limit cycle/fixed point. These detailed analyses are left for our future work.

Acknowledgments

Authors would like to acknowledge Prof. K. Itoh for discussions. Work is partly supported by Grant-in-Aid for Scientific Research of MoE Japan.

References

[1] R.J. Taylor and F.V. Coronitti, Phys. Rev. Lett. **29**, 34 (1972); D. Grésillon, Y. Kiwamoto, J. Phys. Soc. Jpn. **37**, 466 (1974); F. Doveil and M. Buzzi, Phys. Rev. Lett. **34**, 197 (1975).

[2] M. Matsukuma, K. Kaimoto and Y. Kawai, J. Phys. Soc. Jpn. **69**, 303 (2000).

[3] M. Yagi, S.-I. Itoh, K. Itoh and A. Fukuyama, Chaos **9**, 393 (1999).

[4] T. Fujimoto, M. Yagi and S.-I. Itoh, Journal of Plasma and Fusion Research **75**, 1195 (1999).

[5] M. Yamada and K. Ohkitani, J. Phys. Soc. Jpn. **56**, 4210 (1987).

[6] K. Ohkitani and M. Yamada, Progr. Theor. Phys. **89**, 329 (1989).

[7] M.H. Jensen, G. Paladin and A. Vulpiani, Phys. Rev. A **45**, 7214 (1992).

[8] R. Krishunamulti, J. Fluid Mech. **42**, 295 (1971).

[9] A.N. Kolmogorov, Dokl. Akad. Nauk SSSR **30**, 9 (1941), Dokl. Akad. Nauk SSSR **31**, 538 (1941), Dokl. Akad. Nauk SSSR **32**, 16 (1941) and Dokl. Akad. Nauk SSSR **31**, 99 (1941).

[10] L. Biferale, A. Lambert, R. Lima and G. Paladin, Physica D **80**, 105 (1995).